A novel biochemical oscillator tunable by the volume to surface area ratio

ABSTRACT

We propose a model of a novel post-translational mechanism for driving a biochemical oscillator with a frequency tunable by the volume to surface area ratio. The model exploits membrane localization of lipid-modifying enzymes to produce excitation and relaxation of the concentrations of membrane bound species. By designing the reaction dynamics to depend on the volume to surface area ratio, the period of our oscillator model can be directly tuned through mechanical intervention without any need for engineering the underlying biochemistry. Additionally, other cell processes like self-assembly or bioluminescence can be easily coupled to the oscillator through an adaptor binding interface, opening a wide range of potential applications from timed drug delivery to real-time monitoring of cell growth or shape change. While our study is purely computational and has not yet been experimentally validated, the ability to encode the volume to surface area ratio in the frequency of the oscillations offers a new approach for monitoring the growth and division of synthetic cells, and could be useful in a variety of applications such as biosensors and drug delivery.

INTRODUCTION

Biological oscillators are important across a range of biological systems, synchronizing cell processes to each other and predictable external stimuli. The ability of biological oscillators to temporally coordinate reactions in noisy cellular environments makes them attractive elements for artificial biological circuits and other synthetic applications. Previous examples of engineered oscillators have usually been genetic oscillators such as the represillator(Elowitz & Leibler, 2000), but recent attention has been focused on post-translational protein oscillators for their numerous engineering advantages(Olson & Tabor, 2012). Oscillators driven by fast and reversible post-translational modifications such as phosphorylation have the potential to operate on faster and more flexible time-scales than would be allowed by transcription-translation driven genetic oscillators, and can be directly coupled to protein output behavior like fluorescence(Gao et al., 2018). Interesting work has already been done on this front, such as a recent model of a self-assembly-based posttranslational oscillator, but the toolbox of mechanisms available to engineer these types of dynamics is still limited(Kimchi et al., 2020).

One biological system known to produce phosphorylation-driven spatiotemporal oscillations is phosphoinositide (PIP) regulation in lipid membranes(Xiong et al., 2016). PIPs are membrane lipids important for selective membrane recruitment of proteins, and can be phosphorylated or dephosphorylated by lipid-modifying enzymes into a variety of PIP species(Di Paolo & De Camilli, 2006). By controlling the local composition of these PIP species in the lipid membrane the cell can tune the membrane specificity for various protein complexes. As the enzymes controlling the phosphorylation state can themselves be membrane localized as a function of the lipid composition(Bairstow et al.,

2006), there exists the potential for nonlinear feedback mechanisms between enzymatic activity and PIP metabolism(Haucke, 2005) that could drive oscillations.

Membrane localization like this can generate nonlinear feedback because it selectively accelerates reactions and assembly by enhancing the effective binding affinity of reactants on the membrane. This effect is explained by both a reduced diffusive search space in 2D vs 3D, as well as increased effective concentration with the same reactant copy numbers in the lower dimensional space. The effective binding enhancement has been mathematically modeled in recent work by Osman et al as a function of the volume to surface area ratio (V/A) of the system, which scales the forward kinetics of biomolecular reactions(Yogurtcu & Johnson, 2018). According to their analysis using a physiological realistic range of cell V/A, bimolecular kinetics can be enhanced by multiple orders of magnitude compared to their counterparts in 3D diffusive space. Membrane localization is not a static binding enhancement, but rather is regulated by the activity of the previously mentioned lipid-modifying enzymes. Through dynamically tuning the lipid composition, cells have spatiotemporal control of specific membrane-protein affinities to allow encoding of complex molecular logic and spatiotemporal memory in the lipid membrane.

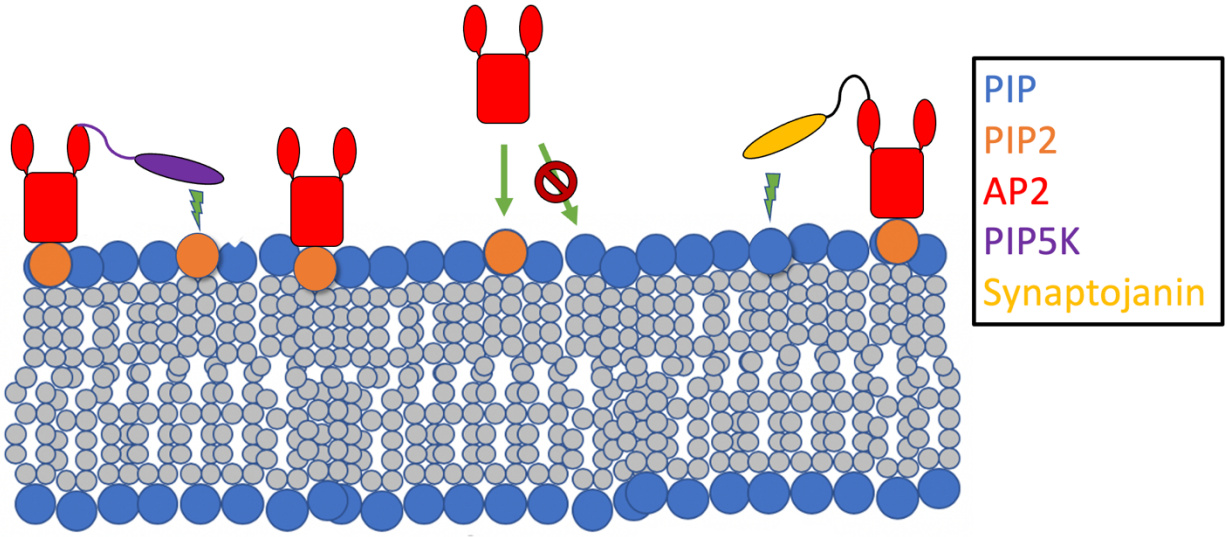

Given the potential of a global variable like the membrane lipid composition to coordinate reaction dynamics, which is tunable by geometric rather than biochemical properties, we sought to build a minimal general model for a biochemical oscillator driven by membrane localization. Our inspiration and general reaction scheme was drawn from the PIP-mediated process of clathrin-mediated endocytosis (CME), where dynamically tuned membrane localization of endocytic machinery is necessary to control the expensive process of clathrin-coat assembly. In CME, the phosphorylated lipid PIP2 is effectively the “on” switch by which the cell signals rapid recruitment of the endocytic machinery for cargo uptake. This recruitment signal is conveyed via the adaptor protein AP2, which has multiple PIP2 specific lipid binding interfaces and protein binding interfaces to indirectly localize CME proteins to the membrane. Like other biological switches, a positive feedback loop exists to discretize concentrations into binary logic: the kinase PIP5K accelerates its own activity through increasing the amount of PIP2 anchors, and the

phosphatase synaptojanin utilizes to amplify its conversion of PIP2 back to PIP for the eventual “off” signal. Through the activity of lipid-modifying kinases and phosphatases, the amount of PIP2 in the membrane can be adjust to either side of the bistable threshold to trigger assembly or disassembly of the clathrin coat.

Generalizing from these basic mechanisms of clathrin-coat assembly, we propose a simple model for a biochemical oscillator that exploits the mechanism of dynamically tuned membrane localization to produce the requisite nonlinearities for oscillations. Our model consists of 5 initial species mapped from CME that interact on and off the membrane with total mass conserved. Two enzymes, a lipid modifying kinase and phosphatase, work in opposition to regulate the dynamic phosphorylation state of the membrane. This membrane is modeled as a mix of phosphorylated PIP2, which facilitates membrane localization of cytosolic proteins, and the unphosphorylated PIP, which doesn’t. The degree of membrane localization, and concomitant binding enhancement conferred to localized proteins, is determined by the ratio of PIP2 to PIP at any given time. Membrane localization of the enzymes occurs indirectly through an adaptor protein AP2, which has lipid binding interface specific to PIP2.

The model possesses oscillatory potential for two reasons. Firstly, the enzymes control the degree of membrane localization, and binding enhancement, for all species in the system, including the enzymes themselves. This means that enzymes accelerate or decelerate their own activity as a function of their dynamic equilibrium on the membrane, producing ad-hoc cooperativity and nonlinear feedback in the form of a symmetrical positive and negative feedback loop. Secondly, this nonlinear feedback is mediated through an intermediate adaptor protein. Intermediates are necessary to delay the feedback so that oscillatory overshoot and undershoot of the steady state is possible. Additionally, the adaptor intermediate feeds the input (PIP2/PIP ratio) incoherently to both enzymes, which has been shown to enhance oscillatory robustness. In summary, high PIP2 concentration recruits more adaptor to the membrane, which recruits both kinase and phosphatase. Kinase binding affinity is enhanced in 2D search space and converts more PIP into PIP2, causing more recruitment through positive feedback. Phosphatase experiences the same enhancement, reducing the amount of PIP2 and membrane localization and using the momentum from the positive feedback to amplify the negative regulation. Through correct tuning of the strength of these two feedbacks (positive feedback must happen faster than negative feedback), the system produces periodic excitation and relaxation in the concentrations of all species.

To characterize the dynamical properties of our oscillatory model and evaluate its experimental realizability, the body of our study is organized as follows: describe the viable oscillatory parameter space as informed by biologically realistic kinetic parameters; explain model reductions and analysis; interrogate the period and amplitude tunability; measure parametric and noise robustness; compare nonspatial modeling results to spatial RD simulation; and finally, discussion of significance/relevance to experimental synthetic biologists.

METHODS

2.1 Chemical Mass Action Kinetics and Nonlinear ODE Formulation

We formulated the model reactions using chemical mass action kinetics, a widely accepted framework for modeling biochemical reaction systems. This approach describes the reaction rate as a product of the reactant concentrations raised to the power of their stoichiometric coefficients. In the nonspatial simulations, we made the typical assumption of mass action, while also incorporating additional assumptions specific to modeling the membrane localization effect. For the membrane localization, 2D versions of 3D reactions have their forward rate constant scaled by volume-to-area ratio divided by a length scale to make it dimensionless. We represented the reaction system as a set of nonlinear ordinary differential equations (ODEs), capturing the dynamic behavior of the system over time. No Michaelis-Menten or steady-state approximations were made for the fully explicit model used for optimization, but were used in a reduced order model to facilitate stability analysis.

2.2 Parameter Optimization using Genetic Algorithm

To ensure stable oscillation periods, we optimized the model parameters using a genetic algorithm (GA). GAs are a class of optimization algorithms inspired by the process of natural selection, which evolve a population of candidate solutions towards an optimal or near-optimal solution. The genetic algorithm optimization allowed all parameters and initial conditions to vary within physiological ranges (though subsets were fixed for certain downstream analyses of solution space). By iteratively applying selection, crossover, and mutation operators, we were able to efficiently search the parameter space and identify a set of model parameters that yielded the desired oscillatory behavior. The optimization process involved 10 generations of 5-30,000 individual parameter vectors.

2.3 Stochastic Simulation using Gillespie Algorithm

To account for the inherently stochastic nature of biochemical reactions, we employed the Gillespie algorithm for simulating our model. This algorithm is a widely used method for simulating stochastic chemical kinetics, enabling us to capture the probabilistic behavior of the system, which is crucial for understanding the dynamics of the oscillator. The Gillespie algorithm generates a series of reaction events and updates the system state according to the reaction propensities, providing us with a detailed, time-resolved view of the system's evolution.

2.4 Spatial Modeling with NERDSS

To incorporate the spatial aspect of our oscillator model, we used the NERDSS (Nonequilibrium Reaction-Diffusion Self-Assembly Simulator) framework, which is written in C++. NERDSS allows for the tracking of individual molecules in space and time, enabling us to model the effects of molecular localization and diffusion on the system's behavior. This spatial information is particularly relevant for our oscillator model, as the membrane localization of lipid-modifying enzymes plays a significant role in generating the tunable oscillations.

2.5 Oscillatory solution verification and classification

While the continuous range of the cost function is useful for optimization and allows iterative convergence, it can produce false positives with poorly behaved solutions (typically concentrations that spike extremely fast from their initial condition but then plateau). So to verify the synthetic datasets

used for downstream analysis, we used a binary classifier to filter out these spurious datapoints and robustly discriminate between oscillatory and non-oscillatory solutions.

2.6 Supplementary Material: Python, Julia, and NERDSS Code

To ensure reproducibility and enable further exploration of our model, we have provided Python, Julia, and NERDSS code in the supplementary material. These codes include the implementation of the model reactions, parameter optimization, Gillespie algorithm simulation, and spatial modeling with NERDSS, allowing other researchers to build upon our work and apply the model to new contexts and applications. The Python and Julia codes make use of their associated analysis libraries for the computational tasks in this study.

RESULTS

Membrane-localization oscillator was designed for experimental feasibility

2D enhancement can be modeled as dimensionless scaling of forward rate constants

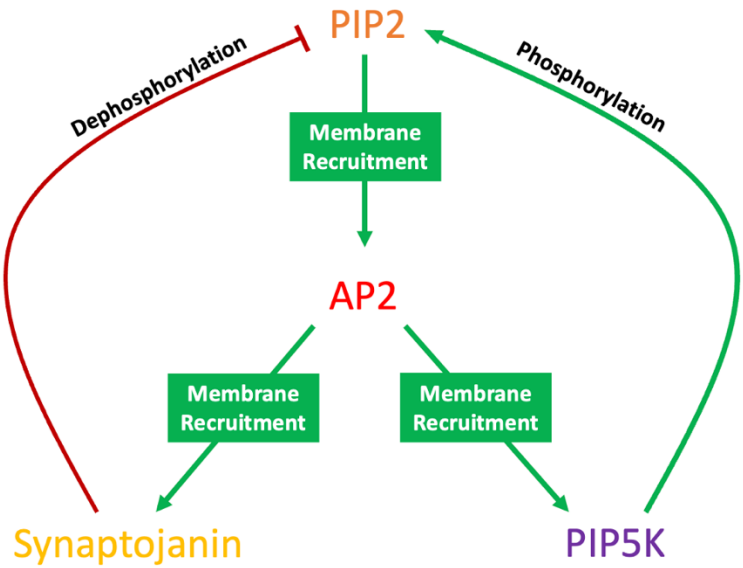

Figure 1: Schematic diagram of the model reactions and species. The model consists of five initial species: a lipid-modifying kinase (K), a lipid-modifying phosphatase (P), an adaptor protein (A), and two lipid species (PIP and PIP2). The lipid species are either bound to the membrane (M) or free in the cytosol ©. The adaptor protein binds to PIP2 on the membrane and recruits the kinase and the phosphatase. The kinase converts PIP to PIP2, while the phosphatase converts PIP2 to PIP. The membrane localization of the species depends on the ratio of PIP2 to PIP, which is controlled by the volume to surface area ratio (V/A) of the cell. The model exhibits oscillatory behavior due to the positive and negative feedback loops between the lipid composition and the enzymatic activity.

Our model primarily consists of a set of 12 coupled ordinary differential equations (ODEs). In order to more rigorously test the oscillatory potential of the model, we initially make no Michaelis-Menten nor quasi-steady state approximations and leave the 12 dimensional system in its expanded form. Within this system, the rates of some species are the sum of both the 3D-2D reaction kinetics ($k_{on} * X * Y$) as well as the same reaction with 2D-2D kinetics ($Df * k_{on} * X * Y$), where the dimensional scaling factor $Df = V/Ah$. This factor weights the feedback strength for both the positive and negative feedback loops, where a higher Df translates to a larger rate enhancement for membrane-localized reactions.

Parameters limited to experimentally realizable ranges

As our goal is to accurately model a synthetic yet still biologically constrained system, our downstream analysis only considers binding and catalytic rates appropriate to our species. The affinity of AP2 for PIP2

(SPR) has been experimentally measured to 0.7 x 10^{2} M^{-1} x s^{-1} for k_{on} and 3.8 x 10^{-2} for k_{off}, according to surface plasmon resonance (SPR) (Höning et al., 2005).

3.1 Oscillator Model and Parameter Optimization

We utilized a genetic algorithm to optimize our nonlinear oscillator model with high reliability. This allowed us to rapidly explore the parameter space and identify sets of model parameters that resulted in stable oscillatory behavior. Analysis of the optimized solutions data revealed that certain parameter combinations, or "sweet spots," consistently produced robust and tunable oscillations; “dead zones” were also observed, where fixing certain combinations of parameters or initial conditions precluded any solutions being found.

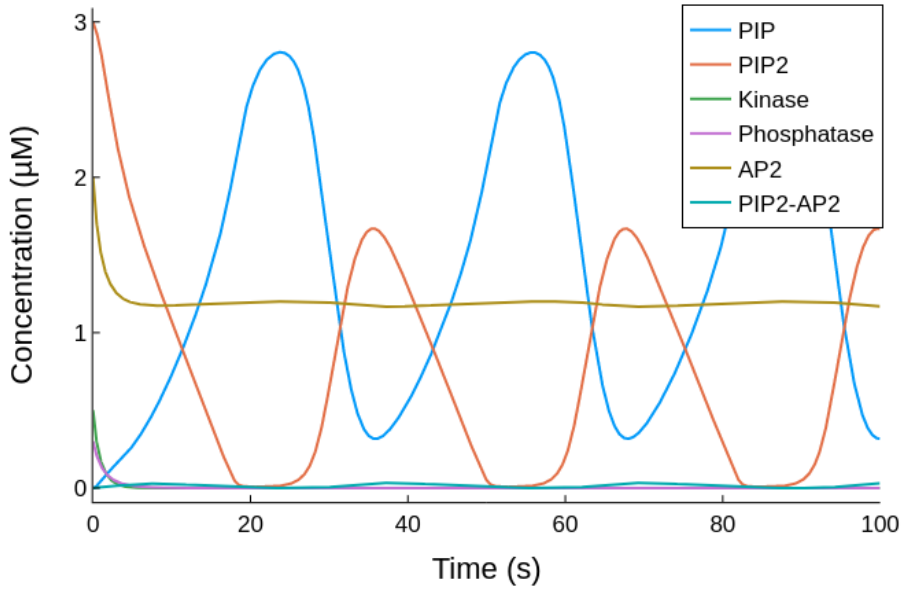

Figure 2: Oscillator Model and Parameter Optimization Results. This figure should display the optimized model parameters and the resulting oscillatory behavior, highlighting the stability of the oscillator over time.

3.2 Tunability of Oscillation Frequency

Our analysis of the novel biochemical oscillator demonstrates a remarkable degree of tunability in the oscillation frequency as a function of the cell's volume-to-surface-area (V/A) ratio. By systematically varying the V/A ratio, we uncovered a unique relationship between this geometric property and the frequency of the oscillations, which has significant implications for the design and implementation of tunable oscillators in synthetic biology.

A key finding in our study is the observation that closed orbits in phase diagrams, with concentrations on the axes, become smaller as the V/A ratio increases. This trend indicates that the oscillation frequency is directly influenced by the cell's geometric properties. To further elucidate this relationship, we calculated the period of oscillation as a function of the V/A ratio, revealing a strong correlation between the two parameters.

Additionally, we explored other phase spaces to visualize and quantify the tunability of our oscillator model. By examining the relationship between enzyme concentrations and lipid-modifying reactions in different phase spaces, we uncovered intricate dynamics that underlie the oscillator's tunable behavior. This comprehensive analysis of phase spaces enables us to identify the key factors that contribute to the oscillator's tunability and understand the underlying mechanisms at play.

To quantitatively assess the tunability of the oscillator, we calculated a tunability index, which measures the change in oscillation frequency as a function of the V/A ratio. Our results demonstrate a highly tunable system, with the oscillator's frequency exhibiting significant sensitivity to changes in the geometric parameter.

Figure 2: Tunability of Oscillation Frequency. This figure should include multiple panels to showcase the various aspects of our investigation into the oscillator's tunability. Panel A could display the phase diagrams with concentrations on the axes, using a colormap to represent the V/A ratio and highlighting the shrinking closed orbits as the ratio increases. Panel B might present a scatter plot or line graph illustrating the strong correlation between the V/A ratio and the period of oscillation. Panel C could showcase selected phase spaces that reveal the intricate dynamics underlying the oscillator's tunable behavior. Finally, Panel D might provide a bar chart or line graph demonstrating the tunability index as a function of the V/A ratio, emphasizing the oscillator's sensitivity to changes in the geometric parameter.

3.3 Stochastic Dynamics of the Oscillator

Our investigation of the stochastic dynamics of the biochemical oscillator model reveals that it exhibits remarkable robustness to noise, while the period of oscillation displays sensitivity to fluctuations. This section provides a comprehensive analysis of the oscillator's behavior under both the stochastic simulation algorithm (Gillespie) and the spatially resolved NERDSS model, enabling us to gain deeper insights into the impact of noise on the system's dynamics.

We initially conducted a qualitative comparison of the model's behavior under different simulation approaches. Our findings indicate that the oscillator can maintain its stable oscillatory behavior even in the presence of noise, with the solutions being recapitulated by both the Gillespie and NERDSS models. This robustness to noise is an essential property for a tunable oscillator and demonstrates its potential applicability in synthetic biology, where the system may be subjected to various sources of noise.

Despite this robustness, our analysis reveals that the period of oscillation is often subject to major fluctuations due to noise. We observed that the magnitude of these fluctuations and discrepancies from the ODE solution is determined by the strength of the positive feedback in the system. This positive feedback is governed by the combined interactions of kcat rate values and the V/A ratio. By systematically exploring the effects of these parameters on the period fluctuations, we were able to identify conditions under which the oscillator displays greater resilience to noise-induced perturbations in the period.

Figure 3: Robustness to Noise and Stochastic Dynamics of the Oscillator. This figure should consist of multiple panels showcasing the results of our analysis of the oscillator's behavior under stochastic conditions. Panel A could display a representative set of oscillatory trajectories obtained using the Gillespie algorithm, highlighting the robustness of the oscillator to noise. Panel B might present similar oscillatory trajectories obtained using the NERDSS model, demonstrating the consistency of the oscillator's behavior across different simulation approaches. Panel C could provide a heatmap or contour plot illustrating the relationship between the strength of positive feedback (as determined by kcat rate values and the V/A ratio) and the magnitude of period fluctuations, revealing the conditions that confer greater resilience to noise-induced perturbations in the period.

3.4 Spatial Dynamics of the Oscillator using NERDSS

In order to gain a deeper understanding of the spatial dynamics of our oscillator model, we employed the NERDSS simulation framework to study the behavior of the system at a molecular level. Our analysis focused on comparing the solution space of NERDSS with that of nonspatial simulations, as well as exploring the potential emergence of spatial oscillations such as waves on the membrane.

We began by rigorously comparing the solution spaces of the NERDSS and nonspatial simulations across various parameter regimes. This comparison enabled us to identify conditions under which the simpler, nonspatial models can be used as a reliable approximation of the system's behavior. Our results demonstrate that, under certain regimes, the nonspatial simulations can adequately capture the dynamics of the oscillator, while other regimes require the more detailed spatial modeling provided by NERDSS.

Next, we investigated the potential for spatial oscillations to arise from the temporal oscillations observed in our model. By carefully examining the spatial distribution of reactants on the membrane, we uncovered the presence of traveling waves and other spatial patterns that emerge as a result of the system's oscillatory dynamics. These spatial oscillations provide an additional layer of complexity to the behavior of our oscillator model and have potential implications for its applications in synthetic biology.

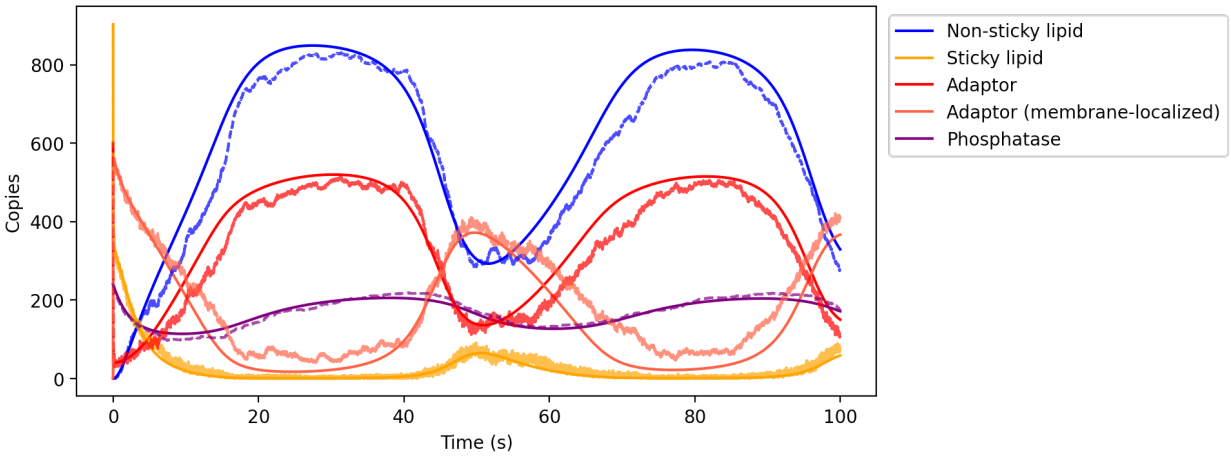

Figure 4: Spatial Dynamics of the Oscillator using NERDSS. This figure should consist of multiple panels illustrating the key findings of our investigation into the spatial dynamics of the oscillator. Panel A could display a heatmap or contour plot comparing the solution spaces of NERDSS and nonspatial simulations across various parameter regimes, highlighting the conditions under which the nonspatial models can be used as a reliable approximation. Panel B might showcase representative snapshots of the spatial distribution of reactants on the membrane at different time points, revealing the emergence of traveling waves and other spatial patterns as a result of the system's oscillatory dynamics.

3.5 Reduced Order Model and Stability Analysis

Our analysis of the biochemical oscillator model led us to develop a reduced order model that significantly simplifies the original system, while still capturing the essential dynamics of the oscillations. Through a series of approximations, we successfully reduced the 12-variable ODE model to a 2-variable system, focusing on the membrane lipid concentrations of PIP and PIP2.

To validate the reduced order model, we performed a comprehensive stability analysis to determine its ability to reproduce the oscillatory behavior observed in the full model. Our results show that the reduced model exhibits oscillations in the PIP and PIP2 concentrations, closely mimicking the dynamics of the original system. This finding demonstrates the utility of the reduced model for analyzing the behavior of the oscillator under various conditions, while significantly reducing the computational complexity.

Furthermore, we conducted a comparative study of the solution spaces for the reduced and full models, revealing a high degree of overlap between the two. This observation indicates that the reduced order model is a reliable and efficient tool for investigating the oscillator's behavior and tunability, particularly in scenarios where computational resources are limited.

Figure 5: Reduced Order Model and Stability Analysis. This figure should consist of multiple panels that highlight the key findings of our investigation into the reduced order model. Panel A could present representative time courses of PIP and PIP2 concentrations for both the full and reduced models, demonstrating the close similarity in their oscillatory dynamics. Panel B might display a heatmap or contour plot comparing the solution spaces of the full and reduced models, emphasizing the high degree of overlap between the two. Panel C could provide a graphical representation of the stability analysis, showcasing the ability of the reduced model to reproduce the oscillatory behavior observed in the full system.

3.6 Visualization of Oscillatory Solutions in Parameter Space

In order to better understand the relationship between the model's parameters and the emergence of oscillations, we investigated the oscillator's behavior within multidimensional parameter spaces. Our approach involved visualizing oscillatory regions in parameter space using contour plots and performing dimensional reduction techniques to gain insights into the system's behavior across different regimes.

We started by plotting contour plots that display oscillatory regions, with the axes representing parameters of interest while keeping all other parameters fixed. These visualizations allowed us to identify how specific parameter combinations give rise to oscillatory behavior in the system. Additionally, we employed dimensional reduction techniques to project the high-dimensional parameter space onto a 2D plane, although the interpretability of these projections was mixed.

To further generalize our understanding of the oscillatory behavior across different fixed regimes, we compared the oscillatory landscapes obtained for various fixed parameter sets. This comparison enabled us to identify common features and trends in the oscillator's behavior as a function of the varied parameters, providing a more comprehensive picture of the system's dynamics.

Another strategy we pursued was the combination of parameters to reduce the dimensionality of the parameter space while preserving the essential features of the oscillatory behavior. This approach allowed us to more effectively visualize and explore the complex parameter dependencies underlying the system's dynamics.

Figure 6: Exploring Oscillatory Solution Landscapes in Multidimensional Parameter Space. This figure should consist of multiple panels showcasing the different techniques employed in our investigation of the oscillator's behavior within multidimensional parameter spaces. Panel A could display representative contour plots depicting oscillatory regions as a function of varied parameters. Panel B might present the results of dimensional reduction techniques, such as projections of the high-dimensional parameter space onto a 2D plane. Panel C could show a comparison of oscillatory landscapes obtained for different fixed parameter sets, highlighting common features and trends in the system's behavior.

3.7 Bifurcation and Robustness Analysis

To assess the robustness and sensitivity of our oscillator model to changes in key parameters, we conducted a bifurcation and robustness analysis. This analysis allowed us to identify critical transitions in the system's dynamics, as well as to evaluate the oscillator's resilience to variations in its governing parameters.

We began by systematically varying one or more parameters of the model, monitoring the system's response to these changes. Our analysis revealed that, for certain parameter combinations, the system exhibits a bifurcation, transitioning from a stable fixed point to sustained oscillations or vice versa. We characterized these bifurcations by tracking changes in the period of oscillations, as well as the amplitude of the oscillatory behavior.

Furthermore, we investigated the oscillator's robustness by introducing perturbations to the system and measuring its ability to maintain stable oscillations. Our results demonstrate that the oscillator is highly robust to moderate perturbations in the parameter values, with the oscillatory behavior persisting even in the presence of significant fluctuations. This finding highlights the potential applicability of our model in synthetic biology contexts, where resilience to environmental variability is crucial.

Figure 7: Bifurcation and Robustness Analysis of the Oscillator Model. This figure should consist of multiple panels illustrating the key findings of our bifurcation and robustness analysis. Panel A could display a bifurcation diagram, with the varied parameter on the x-axis and the period of oscillations on the y-axis, showcasing the transitions between different dynamical regimes as the parameter is varied. Panel B might present a representative time course of the oscillator's behavior in response to perturbations, demonstrating the system's ability to maintain stable oscillations despite fluctuations in parameter values. Panel C could provide a heatmap or contour plot illustrating the oscillator's resilience across a range of parameter combinations, highlighting regions of high robustness in the parameter space.

3.8: Sensitivity to Particular Parameters

To better understand the key parameters and initial conditions driving the behavior of our oscillator model, we conducted both global and local sensitivity analyses. These analyses allowed us to identify the most influential parameters and initial conditions with respect to various properties of the oscillatory behavior, such as oscillatory score, amplitude, and period.

Our global sensitivity analysis employed the Sobol method, which quantifies the contribution of individual parameters and their interactions to the overall variance of the model output. Our findings revealed that ka1, kb4, and V/A were the most important parameters governing the oscillator's behavior, while the initial concentration of AP2 was identified as the most influential initial condition. To

visualize these results more effectively, we generated a heatmap representation of the total sensitivity indices, showcasing the relative importance of each parameter and initial condition.

In addition to the global analysis, we also performed a local sensitivity analysis, which assessed the impact of small variations in the parameters and initial conditions on the system's behavior. By calculating partial derivatives of the oscillator's properties with respect to the parameters, we identified regions of high sensitivity in the parameter space. These findings complemented the global sensitivity analysis, offering a more detailed picture of how the oscillator responds to changes in its governing parameters and initial conditions.

Figure 8: Sensitivity Analysis of the Oscillator Model. This figure should consist of multiple panels illustrating the results of our global and local sensitivity analyses. Panel A could display a heatmap representation of the total sensitivity indices obtained from the Sobol global sensitivity analysis, highlighting the relative importance of each parameter and initial condition. Panel B might present the results of the local sensitivity analysis, showcasing regions of high sensitivity in the parameter space, with contour lines or color gradients representing the magnitude of the partial derivatives. Panel C could offer a side-by-side comparison of the most influential parameters identified in both global and local analyses, providing a comprehensive overview of the key drivers of the oscillator's behavior.

3.9: Comparison with Other Biochemical Oscillators

To contextualize our findings and demonstrate the potential advantages of our proposed post-translational oscillator model, we performed a comparative analysis with other biochemical oscillators, including a well-known genetic oscillator and another synthetic post-translational protein oscillator. This comparison allowed us to highlight the unique features and benefits of our model, as well as to assess its potential for experimental realization.

We first compared our oscillator model with a classic genetic oscillator, such as the repressilator. Our analysis showed that our post-translational oscillator exhibits faster response times due to the absence of transcription and translation steps, resulting in a more rapid synchronization of cellular processes. Moreover, our model's reliance on lipid-modifying enzymes and membrane localization confers greater tunability and adaptability to changes in the cell's geometric properties.

Next, we contrasted our model with another synthetic post-translational protein oscillator from the literature. We found that our model demonstrates increased robustness to noise, as well as greater tunability in terms of oscillation frequency. Furthermore, our model offers the potential for spatial oscillations, which could give rise to membrane-bound waves and other intriguing spatiotemporal dynamics.

Finally, we assessed the potential experimental performance of our model by examining the relationship between model behavior and experimental data for the other oscillators. By extrapolating these relationships, we could infer the likely experimental characteristics of our oscillator, such as its robustness, tunability, and the extent to which it may be amenable to experimental manipulation.

Figure 9: Comparison with Other Biochemical Oscillators. This figure should consist of multiple panels illustrating the key differences and advantages of our oscillator model compared to other biochemical oscillators. Panel A could depict a side-by-side comparison of the oscillatory behavior of our model and a genetic oscillator, emphasizing the faster response times and tunability of our model. Panel B might showcase a comparison with another synthetic post-translational protein oscillator, highlighting our model's increased robustness, tunability, and potential for spatial oscillations. Panel C could present an extrapolation of the experimental performance of our model based on the relationship between model behavior and experimental data for other oscillators, providing insights into its potential for experimental realization.

DISCUSSION

In this study, we presented a minimal general model for a biochemical oscillator driven by dynamically tuned membrane localization, inspired by the process of clathrin-mediated endocytosis (CME). Our model exploited the mechanism of membrane localization to produce the requisite nonlinearities for oscillations, with the frequency of the oscillations tunable by the volume to surface area (V/A) ratio. This tunability allows for direct control of the oscillator's period through mechanical intervention, without the need for engineering the underlying biochemistry.

By comparing our model with other biochemical oscillators, we highlighted its advantages, such as its robustness to noise, flexibility in tunability, and potential applications in timed drug delivery and real-time monitoring of cell growth or shape change. The results of our analyses demonstrated the oscillator's performance in various parameter regimes, sensitivity to key parameters and initial conditions, and its behavior in both spatial and non-spatial contexts.

Despite the promising findings, several outstanding questions and areas for further exploration remain. First, experimental validation of the proposed model is crucial. It would be interesting to test the model in vivo, employing synthetic biology techniques to construct the oscillator system and validate the predicted behavior in a controlled environment.

Second, a more detailed investigation of the role of specific reaction mechanisms and parameters is necessary to understand the oscillator's behavior better. This could involve a deeper exploration of the model's robustness under different conditions or the inclusion of additional layers of regulation and feedback to study their impact on the system's performance.

Third, expanding the model to incorporate other cellular processes, such as self-assembly or bioluminescence, could help investigate potential applications in biosensing, drug delivery, and monitoring of cell growth or shape change. By coupling these processes to the oscillator through an adaptor binding interface, a wide range of possibilities for synthetic biology applications could be explored.

In conclusion, the proposed oscillator model offers a novel approach to driving biochemical oscillations by exploiting membrane localization and tunability of the V/A ratio. This model has the potential to impact a wide range of applications in synthetic biology, including biosensors and drug delivery. Further investigation and experimental validation are necessary to fully understand the model's potential and limitations and to pave the way for its application in various contexts.

DRAFT NOTES

1. Experimentally realizable parameter ranges for binding and catalysis

2. Is this system minimal or can AP2 be reduced out of model? Probably not, but talk about why

3. Compare requisite relative strengths of positive and negative feedback, membrane localization

4. Tunability in physiological parameter space vs. Clathrin protein specific parameter space

REFERENCES

Bairstow, S. F., Ling, K., Su, X., Firestone, A. J., Carbonara, C., & Anderson, R. A. (2006). Type Iγ661 Phosphatidylinositol Phosphate Kinase Directly Interacts with AP2 and Regulates Endocytosis. *Journal of Biological Chemistry*, *281*(29), 20632-20642. https://doi.org/10.1074/jbc.m601465200

Di Paolo, G., & De Camilli, P. (2006). Phosphoinositides in cell regulation and membrane dynamics. *Nature*, *443*(7112), 651-657. https://doi.org/10.1038/nature05185

Elowitz, M. B., & Leibler, S. (2000). A synthetic oscillatory network of transcriptional regulators. *Nature*, *403*(6767), 335-338. https://doi.org/10.1038/35002125

Gao, X. J., Chong, L. S., Kim, M. S., & Elowitz, M. B. (2018). Programmable protein circuits in living cells. *Science*, *361*(6408), 1252-1258. https://doi.org/10.1126/science.aat5062

Haucke, V. (2005). Phosphoinositide regulation of clathrin-mediated endocytosis. *Biochem Soc Trans*, *33*(Pt 6), 1285-1289. https://doi.org/10.1042/BST0331285

Höning, S., Ricotta, D., Krauss, M., Späte, K., Spolaore, B., Motley, A., Robinson, M., Robinson, C., Haucke, V., & Owen, D. J. (2005). Phosphatidylinositol-(4,5)-Bisphosphate Regulates Sorting Signal Recognition by the Clathrin-Associated Adaptor Complex AP2. *Molecular Cell*, *18*(5), 519-531. https://doi.org/10.1016/j.molcel.2005.04.019

Kimchi, O., Goodrich, C. P., Courbet, A., Curatolo, A. I., Woodall, N. B., Baker, D., & Brenner, M. P. (2020). Self-assembly–based posttranslational protein oscillators. *Science Advances*, *6*(51), eabc1939. https://doi.org/10.1126/sciadv.abc1939

Olson, E. J., & Tabor, J. J. (2012). Post-translational tools expand the scope of synthetic biology. *Curr Opin Chem Biol*, *16*(3-4), 300-306. https://doi.org/10.1016/j.cbpa.2012.06.003

Xiong, D., Xiao, S., Guo, S., Lin, Q., Nakatsu, F., & Wu, M. (2016). Frequency and amplitude control of cortical oscillations by phosphoinositide waves. *Nature Chemical Biology*, *12*(3), 159-166. https://doi.org/10.1038/nchembio.2000

Yogurtcu, O. N., & Johnson, M. E. (2018). Cytosolic proteins can exploit membrane localization to trigger functional assembly. *PLOS Computational Biology*, *14*(3), e1006031. https://doi.org/10.1371/journal.pcbi.1006031